DOI: 10.1002/ange.201210090

Self-Assembly

Supramolecular Thiophene Nanosheets**

*Yijun Zheng, Haixin Zhou, Dian Liu, George Floudas, Manfred Wagner, Kaloian Koynov, Markus Mezger, Hans-Jürgen Butt, and Taichi Ikeda**

Recently, two-dimensional (2D) materials, like graphene,[1] inorganic nanosheets,[2] 2D polymers etc.,[3] attract much attention owing to their unique structure and potential applications for nanodevices. These membranes have molecular-scale thickness (less than 5 nm) with huge surface areas, which offer ample scope for further fabrication or modification.[4] Self-assembled supramolecular nanosheets are also attractive, because their constituents are not crosslinked covalently, which makes it possible to control the size and shape of the self-assembled structure by environmental conditions.[5] Many examples of self-assembled nanosheets have been reported including the lamellar structure of hydrogen-bonding gelators,[6] amphiphilic or phase-segregated block copolymers.[7] In those previous studies, the molecules and block copolymers were designed to have a plethora of molecular interactions, which directly lead to the formation of the sheet structure. In contrast, biological systems, that is, proteins, adopt a more complex hierarchical approach. The polypeptides are folded with the help of secondary structures (α-helices and β-sheets) and subsequently organized into higher-order structures, such as fibers and nanosheets.[8] Achieving a hierarchical self-assembly by using artificial polymer folding is still challenging.[9]

Artificial polymer folding has been achieved by using copolymers consisting of a rigid aromatic unit and a flexible oligo(ethylene glycol) (OEG) unit.[10,11] We applied phenyl-capped bithiophene (Ph2TPh) as a rigid unit (poly(Ph2TPh-OEG), Figure 1a), because the Ph2TPh unit has a high crystallinity[12] and a potential for the application in molecular electronics.[13] A similar molecular design was reported by some research groups.[14] O. Henze et al. reported the fiber formation of OEG-substituted thiophenes,[15] but the copolymer with the same constituents lost the self-assembling ability.[14b] Although S. Okamoto et al. have reported the stacked-sheet structure of the folded copolymer on a substrate,[16] self-assembly of the folded copolymer in solution was unclear. In this study, we found that folded poly(Ph2TPh-OEG) forms supramolecular nanosheets in some organic solvents. Interestingly, the monomer unit, Ph2TPh-alkyne (Figure 1a), did not form well-defined self-assembled structures under the same conditions. This result indicates that the folding of the copolymer is a key step to form higher-order structures, which mimics natures' strategy. We successfully modified the nanosheet surface with a fluorescent probe and observed the suspended nanosheets in solution.

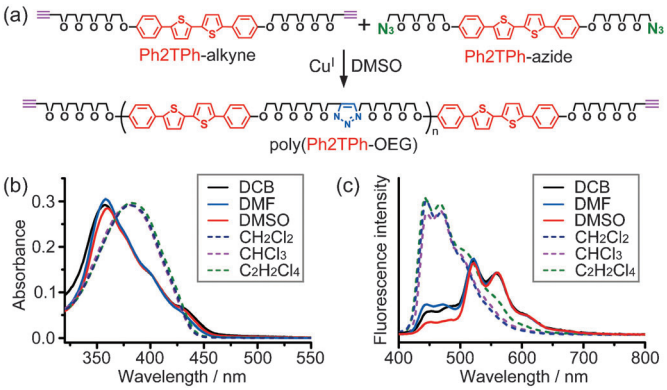

Figure 1. a) Synthesis of copolymer poly(Ph2TPh-OEG). b) Solvent-dependent UV/Vis spectra of poly(Ph2TPh-OEG). Concentration of the Ph2TPh unit: 1.0×10^{-5} M. c) Solvent-dependent fluorescence spectra of poly(Ph2TPh-OEG). Concentration of the Ph2TPh unit: 3×10^{-6} M. Excitation wavelength is 365 nm.

Poly(Ph2TPh-OEG) was synthesized by copper(I)-catalyzed azide–alkyne Huisgen cycloaddition of the alkyne- and azido-functionalized monomers Ph2TPh-alkyne and Ph2TPh-azide. (Figure 1a).[17] The feed ratio of Ph2TPh-alkyne/Ph2TPh-azide was 1.0:0.9 so that most of the copolymers have acetylene terminal groups. The chemical structure and molecular weight of the copolymer were characterized by ^{1}H NMR spectroscopy (Figure S4 in the Supporting Information) and gel-permeation chromatography (GPC), respectively (Figure S5, $M_n = 1.6\times10^4$ Da, $M_w/M_n = 3.5$).

Solvent-dependent UV/Vis absorption spectra of poly(Ph2TPh-OEG) were measured. In dichloromethane, chloroform, and 1,1,2,2-tetrachloroethane, poly(Ph2TPh-OEG) gave a smooth single absorption peak around 380 nm. Since these spectra are comparable to that of the monomer unit Ph2TPh-alkyne (Figure 1b and Figure S6a in the Supporting Information), the absorption at 380 nm is assigned to the

[*] Dr. Y. Zheng, H. Zhou, Dr. D. Liu, Prof. Dr. G. Floudas, Dr. M. Wagner, Dr. K. Koynov, Dr. M. Mezger, Prof. Dr. H.-J. Butt, Dr. T. Ikeda
Max Planck Institute for Polymer Research (MPIP)
Ackermannweg 10, 55128 Mainz (Germany)
Prof. Dr. G. Floudas
Department of Physics, University of Ioannina
45110 Ioannina (Greece)
Dr. T. Ikeda
Polymer Materials Unit
National Institute for Materials Science (NIMS)
Namiki 1-1 Tsukuba 305-0044 (Japan)
E-mail: IKEDA.Taichi@nims.go.jp

[**] We acknowledge the discussions with Prof. Dr. Werner Steffen, and we thank Christine Rosenauer for GPC, Thiel Jürgen for DSC and TGA, and Andreas Best for confocal microscope imaging experiments.

Supporting information for this article is available on the WWW under http://dx.doi.org/10.1002/anie.201210090.

© 2013 Wiley-VCH Verlag GmbH & Co. KGaA, Weinheim

dispersed Ph2TPh unit. In contrast, poly(Ph2TPh-OEG) in 1,2-dichlorobenzene (DCB), *N*,*N*′-dimethylformamide (DMF), and dimethylsulfoxide (DMSO) showed blue-shifted peaks around 360 nm, which are assigned to the aggregated Ph2TPh units.[15,18] Fluorescence spectra support the above assignments. Namely, poly(Ph2TPh-OEG) displays monomer emission in CH_2Cl_2, $CHCl_3$, and $C_2H_2Cl_4$, but excimer emission in DCB, DMF, and DMSO (Figure 1c).[16] Spectra of the monomer unit Ph2TPh-alkyne did not depend on the solvent (Figure S6a). These results indicate that the polymeric structure is the key for inducing the aggregation of Ph2TPh units.

To characterize the association behavior of Ph2TPh units in more detail, we conducted temperature-dependent UV/Vis spectra measurements at three different concentrations in DCB (Figure S7 in the Supporting Information). With increasing temperature, the absorption peak of the aggregated Ph2TPh units decreased, whereas the peak of the dispersed Ph2TPh units increased. This process was reversible (Figure S6b). Different sets of isosbestic points were detectable below 100 °C (374 nm and 431 nm) and above 100 °C (365 nm and 437 nm; Figure S7b,c). This result indicates that the system contains two different processes below and above 100 °C. The relationship between the absorption at 358 nm and the temperature (Figure S7f) indicates that the first process below 100 °C is concentration-dependent; the second is not. The former and latter processes are attributed to self-assembly and folding, respectively, because the folding process, which is intramolecular, should be concentration-independent, but the self-assembly, which is intermolecular, should depend on the concentration.[19]

The temperature dependency of the size of the self-assembled structure was confirmed by dynamic light scattering (Figure S8a,b in the Supporting Information) in DCB. The hydrodynamic radius of the self-assembled structure decreased with increasing the temperature from 30 to 80 °C, thus supporting the assignment of the first process below 100 °C to the disassembly of the self-assembled structure. The solvent dependency of the self-assembly process was also confirmed by using the DCB and $CHCl_3$ solutions (Figure S8c,d). In the DCB solution, scattering corresponding to larger matter with a radius of approximately 280 nm was detectable, which disappeared in $CHCl_3$.

Temperature-dependent ^{1}H NMR spectroscopic measurements were conducted in the range from 25 to 80 °C in a $C_2D_2Cl_4$/[D_6]DMSO solvent mixture (Figure S9 in the Supporting Information). The mixed solvent lowers the dissociation temperature of the Ph2TPh units. Although the thiophene aromatic peaks were not observed at low temperature, sharp peaks appeared at higher temperature. This result indicates that the mobility of the Ph2TPh unit would be suppressed at lower temperature owing to the aggregation, which leads to a shorter T_2 relaxation time.

Poly(Ph2TPh-OEG) could self-assemble into sheets in DCB, DMF, and DMSO. The sheet structure was confirmed by transmission electron microscopy (TEM; Figure 2a,b and Figure S10 in the Supporting Information). TEM samples were prepared by putting a droplet of the sample solution on a TEM support, followed by removal of the solution by tilting

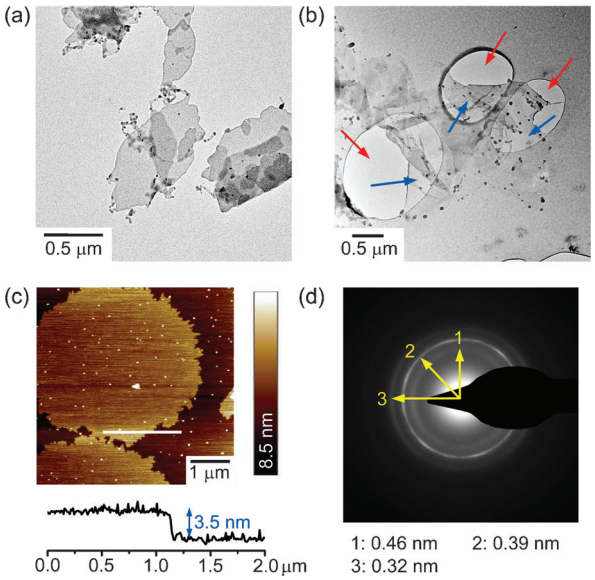

Figure 2. a) TEM image of the self-assembled poly(Ph2TPh-OEG) structure. The sample was prepared by using a DCB solution. Concentration of the Ph2TPh unit: 5.0×10^{-5} M. b) TEM image of self-standing nanosheets (blue arrows) on micropores (red arrows). The sample was prepared by using a DCB solution. Concentration of the Ph2TPh unit: 1.0×10^{-4} M. c) Top left: AFM image of supramolecular thiophene nanosheets on a silicon wafer; top right: height scale bar with the range of height being 8.5 nm; bottom: section profile of the white line in the AFM image. The sample was prepared by using a DCB solution. Concentration of the Ph2TPh unit: 1.0×10^{-4} M. d) Electron diffraction pattern of stacked supramolecular thiophene nanosheets on a carbon support film.

the TEM support. We succeeded to obtain a TEM image of the self-standing sheets by using a perforated carbon support film (Figure 2b). The size of the sheet is comparable to that determined by dynamic light scattering (Figure S8). These results suggest that the sheet structure was formed by self-assembly in solution, not by surface-assisted self-assembly. Poly(Ph2TPh-OEG) did not form well-defined self-assembled structures in CH_2Cl_2, $CHCl_3$, and $C_2H_2Cl_4$ (Figure S10d,e,f in the Supporting Information).

To measure the thickness of the sheets, we applied atomic force microscopy. It was confirmed that the self-assembled sheet has a homogenous height of 3.5 nm and micrometer lateral size (Figure 2c). The size of these nanosheets depends on the concentration of the solution (Figure S11 in the Supporting Information). At a concentration of 1×10^{-4} M, large sheets over several μm and some stacked sheets were observable (Figure S11c,d). Since large nanosheets tend to form stacks in solution, a further increase in the concentration resulted in a gel consisting of stacked nanosheets. The monomer Ph2TPh-alkyne did not self-assemble into well-defined structures under the same condition.

Wide-angle X-ray scattering (WAXS) measurements were conducted by using a solid powder sample of the nanosheets prepared by lyophilization of DCB solution (Figure 3a). At low angles, a set of two broad reflections (first order at $2\theta = 2.34°$, second order at 4.66°) indicates a lamellar structure with a periodicity of 3.5 nm. The *d* spacing of 3.5 nm agrees well with the thickness of the nanosheet

© 2013 Wiley-VCH Verlag GmbH & Co. KGaA, Weinheim

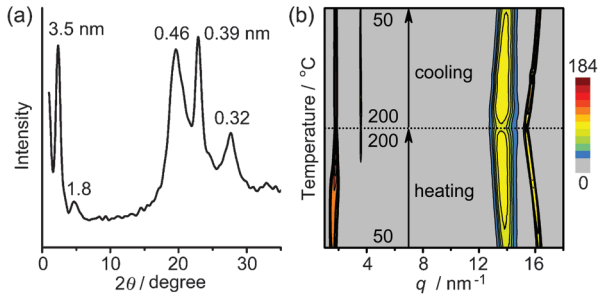

Figure 3. a) Wide-angle X-ray scattering pattern of a self-assembled poly(Ph2TPh-OEG) powder sample in the solid state. The corresponding *d* spacing values in nm are given next to the peaks. b) WAXS isointensity contour plots as a function of temperature. The color scale corresponds to intensity.

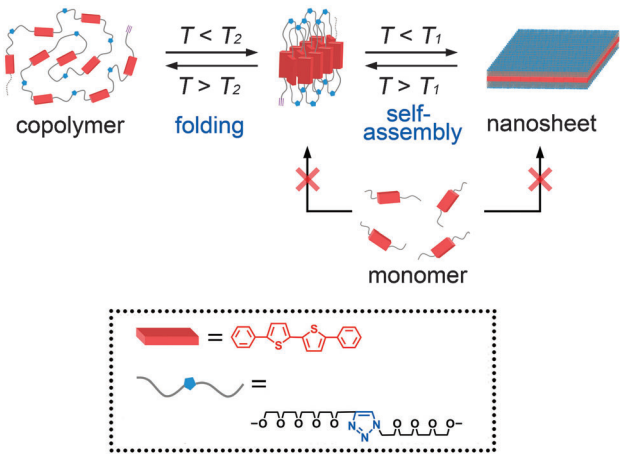

Figure 4. Illustration of a proposed mechanism for the formation of supramolecular thiophene nanosheets. T_1: Dissociation temperature of the nanosheets, T_2: unfolding temperature of the copolymer. $T_1 < T_2$.

determined by AFM. This result suggests that the self-assembled nanosheets maintain their structure in the powder samples. The thickness of the single layer (3.5 nm) is smaller than the expected length of the repeating unit (ca. 4.0 nm, estimated from the crystal structures of poly(ethylene glycol),[20] $1.948 \times (4/7) \times 2 = 2.23$ nm, and the Ph2TPh unit,[13a] 1.78 nm). This deviation may originate from a low crystallinity of OEG chains or tilting of the OEG chains against the long axis of the Ph2TPh unit[13a] and even both.

At higher angles, we observed three broad diffraction peaks corresponding to the *d* spacings of 0.46, 0.39, and 0.32 nm. An electron diffraction measurement of the stacked nanosheets (Figure 2d) indicates that these peaks are associated with the in-plane structure that is, the molecular packing of the Ph2TPh units within the nanosheets. Since this WAXS pattern is comparable to that observed in a vacuum-evaporated sexithiophene film,[21] these peaks are tentatively assigned to the (110), (020), and (120) reflexes of a herringbone structure (orthogonal, $a = 0.57$ nm, $b = 0.78$ nm, Figure S12 in the Supporting Information). However, it is impossible to determine the accurate atomic positions of the Ph2TPh units owing to the low crystallinity and the small number of significant reflections.

The result of the temperature-dependent WAXS measurement is shown in Figure 3b. Although a slight decrease of the scattering intensity was detectable above 180 °C, the ordered structure persisted up to high temperatures. The result of differential scanning calorimetry (DSC) indicated that poly(Ph2TPh-OEG) starts to melt above 180 °C (Figure S13b in the Supporting Information). The thermal decomposition temperature (5 wt % loss) was found to be 375 °C by thermogravimetric analysis (Figure S13a). However, a color change of the sample was detectable after the annealing at 180 °C for 24 h (Figure S14 in the Supporting Information). The ^{1}H NMR spectrum of the annealed sample indicated a slight deterioration of the Ph2TPh unit.

Figure 4 shows a model for the formation of supramolecular thiophene nanosheets. The homogeneous thickness of the nanosheets (3.5 nm) and 2D molecular packing structure derived from the diffraction patterns (Figure S12 in the Supporting Information) support the folded conformation of the copolymer in the nanosheet. There is an equilibrium between the free copolymer and the self-assembled nanosheet. AFM measurements revealed that the equilibrium strongly depends on the concentration of the solution (Figure S11). Temperature-dependent UV/Vis spectra at different concentrations indicated that the self-assembly and folding are independent processes (Figure S7f). The dissociation temperature of the nanosheet (T_1) is lower than the unfolding temperature of the copolymer (T_2). Although T_1 depends on the concentration of the solution, T_2 is always 110 °C in DCB. This indicates that the folded conformation is quite stable in DCB. Notably, the monomer unit of the copolymer (Ph2TPh-alkyne) could not form well-defined self-assembled structures under the same conditions. It is considered that in the case of Ph2TPh-alkyne, the intermolecular interaction (enthalpy gain) is not strong enough to overcome the entropy loss. In the case of the copolymer, Ph2TPh units are covalently linked. The entropy loss in the folding process of the copolymer should be smaller than that of the self-assembly process of the free monomers in the solution. The copolymer can keep a high local concentration of Ph2TPh units within a single copolymer chain irrespective of the copolymer concentration in the solution. The 1,4-triazole linker also assists to form the hairpin conformation of the OEG chains. Owing to these favorable factors, the folded conformation of the copolymer is stable in DCB, DMF, and DMSO. Compared to the monomer unit Ph2TPh-alkyne, the folded copolymer has a much larger interaction surface with the surrounding copolymers, which leads to further interpolymer association. Solvent-dependent nanosheet formation suggests that the phase segregation of Ph2TPh units from the solvent is an important driving force for inducing the folding and the subsequent nanosheet formation. T-type CH–π interactions between the Ph2TPh units can also stabilize the nanosheet (Figure S12). Although the structure of the single folded copolymer is difficult to determine, it is considered that Ph2TPh units are associated with each other like in Figure 4 so as to maximize the interaction between Ph2TPh units and minimize the interface of Ph2TPh units to the solvent. It was reported that the herringbone arrangement of thiophene/phenylene co-oligomers would induce a blue-shift of the UV/Vis absorption.[22]

The supramolecular thiophene nanosheets reported herein have many acetylene groups on the surface, which allow further chemical modification of the nanosheet sur-

© 2013 Wiley-VCH Verlag GmbH & Co. KGaA, Weinheim

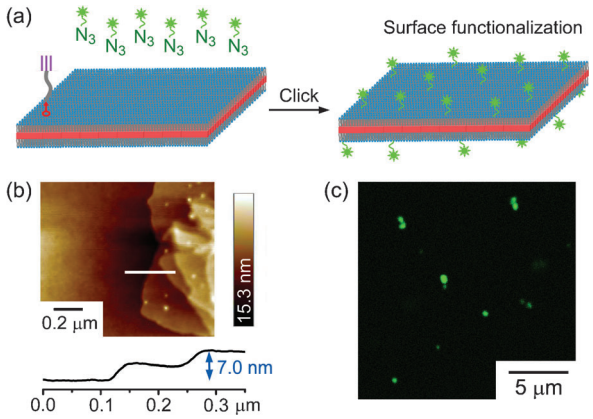

Figure 5. a) Illustration of the chemical modification of the nanosheet surface by a fluorescent probe (Alexa Fluor 488 Azide). b) Top left: AFM image of nanosheets with attached fluorescent probe; top right: scale bar for AFM height; bottom: section profile of the white line in the AFM image. c) Confocal fluorescence microscopy image of suspended dye-attached nanosheets in DMSO. Excitation wavelength: 488 nm.

face.[23] To prove this idea, we introduced a fluorescent probe (Alexa Fluor 488 Azide) on the nanosheet surface by using a Cu^{I}-catalyzed Huisgen cycloaddition (Figure 5a). Unreacted fluorescent probe was removed by dialysis. The covalent attachment of the fluorescent probe to the copolymer was confirmed by thin layer chromatography (Figure S15 in the Supporting Information). From the fluorescence intensity of Alexa Fluor 488 and the integral of the ^{1}H NMR peaks, it was calculated that 85% of the acetylene terminal groups were functionalized by Alexa Fluor 488 Azide (Figure S16 in the Supporting Information). After the attachment of the fluorescent probe, poly(Ph2TPh-OEG) still maintained the nanosheet structure (Figure 5b) as well as emitted the characteristic green fluorescence of Alexa Fluor 488 (Figure 5c), thereby indicating a successful chemical modification of the nanosheet surface without disrupting the self-assembled structure.

In conclusion, supramolecular thiophene nanosheets were prepared by hierarchical self-assembly of the copolymer poly(Ph2TPh-OEG) through artificial polymer folding. The nanosheet formation requires the folding of the copolymer, which is comparable to the protein folding and self-assembly. Since the copolymer has the folded conformation, the thickness of the thiophene nanosheet is only 3.5 nm, which is comparable to that of the lipid bilayer. The lateral size of the nanosheet is controllable by the temperature and concentration of the solution. We also proved that the surface of the nanosheet could be flexibly functionalized by efficient click reaction without disrupting the nanosheet structure. These results may lead to a variety of potential applications, such as optoelectronic devices, solar cells, scaffolds for catalysts, sensors, and biomaterials.

Received: December 18, 2012
Revised: February 6, 2013
Published online: March 26, 2013

Keywords: click chemistry · nanosheets · polymer folding · self-assembly · thiophene derivatives

[1] a) J. C. Meyer, A. K. Geim, M. I. Katsnelson, K. S. Novoselov, T. J. Booth, S. Roth, *Nature* **2007**, *446*, 60–63; b) J. S. Bunch, A. M. van der Zande, S. S. Verbridge, I. W. Frank, D. M. Tanenbaum, J. M. Parpia, H. G. Craighead, P. L. McEuen, *Science* **2007**, *315*, 490–493.
[2] M. Osada, T. Sasaki, *Adv. Mater.* **2012**, *24*, 210–228.
[3] a) X. Feng, X. S. Ding, D. L. Jiang, *Chem. Soc. Rev.* **2012**, *41*, 6010–6022; b) P. Kissel, R. Erni, W. B. Schweizer, M. D. Rossell, B. T. King, T. Bauer, S. Gotzinger, A. D. Schluter, J. Sakamoto, *Nat. Chem.* **2012**, *4*, 287–291.
[4] J. Kim, L. J. Cote, J. X. Huang, *Acc. Chem. Res.* **2012**, *45*, 1356–1364.
[5] a) T. Govindaraju, M. B. Avinash, *Nanoscale* **2012**, *4*, 6102–6117; b) H. J. Kim, T. Kim, M. Lee, *Acc. Chem. Res.* **2011**, *44*, 72–82.
[6] a) T. Seki, Y. Maruya, K. Nakayama, T. Karatsu, A. Kitamura, S. Yagai, *Chem. Commun.* **2011**, *47*, 12447–12449; b) R. Davis, R. Berger, R. Zentel, *Adv. Mater.* **2007**, *19*, 3878–3881.
[7] J. del Barrio, L. Oriol, C. Sanchez, J. L. Serrano, A. Di Cicco, P. Keller, M. H. Li, *J. Am. Chem. Soc.* **2010**, *132*, 3762–3769.
[8] J. W. Bryson, S. F. Betz, H. S. Lu, D. J. Suich, H. X. X. Zhou, K. T. Oneil, W. F. Degrado, *Science* **1995**, *270*, 935–941.
[9] K. T. Nam, S. A. Shelby, P. H. Choi, A. B. Marciel, R. Chen, L. Tan, T. K. Chu, R. A. Mesch, B. C. Lee, M. D. Connolly, C. Kisielowski, R. N. Zuckermann, *Nat. Mater.* **2010**, *9*, 454–460.
[10] A. D. Q. Li, W. Wang, L. Q. Wang, *Chem. Eur. J.* **2003**, *9*, 4594–4601.
[11] T. Muraoka, T. Shima, T. Hamada, M. Morita, M. Takagi, K. Kinbara, *Chem. Commun.* **2011**, *47*, 194–196.
[12] a) M. A. Stokes, R. Kortan, S. R. Amy, H. E. Katz, Y. J. Chabal, C. Kloc, T. Siegrist, *J. Mater. Chem.* **2007**, *17*, 3427–3432; b) J. J. Apperloo, L. Groenendaal, H. Verheyen, M. Jayakannan, R. A. J. Janssen, A. Dkhissi, D. Beljonne, R. Lazzaroni, J. L. Bredas, *Chem. Eur. J.* **2002**, *8*, 2384–2396.
[13] a) J. C. Maunoury, J. R. Howse, M. L. Turner, *Adv. Mater.* **2007**, *19*, 805–809; b) A. Sung, M. M. Ling, M. L. Tang, Z. A. Bao, J. Locklin, *Chem. Mater.* **2007**, *19*, 2342–2351.
[14] a) A. F. M. Kilbinger, W. J. Feast, *J. Mater. Chem.* **2000**, *10*, 1777–1784; b) O. Henze, M. Fransen, P. Jonkheijm, E. W. Meijer, W. J. Feast, A. Schenning, *J. Polym. Sci. Part A* **2003**, *41*, 1737–1743.
[15] P. Leclère, M. Surin, P. Viville, R. Lazzaroni, A. F. M. Kilbinger, O. Henze, W. J. Feast, M. Cavallini, F. Biscarini, A. Schenning, E. W. Meijer, *Chem. Mater.* **2004**, *16*, 4452–4466.
[16] J. Watanabe, T. Hoshino, Y. Nakamura, E. Sakai, S. Okamoto, *Macromolecules* **2010**, *43*, 6562–6569.
[17] V. V. Rostovtsev, L. G. Green, V. V. Fokin, K. B. Sharpless, *Angew. Chem.* **2002**, *114*, 2708–2711; *Angew. Chem. Int. Ed.* **2002**, *41*, 2596–2599.
[18] O. Henze, W. J. Feast, F. Gardebien, P. Jonkheijm, R. Lazzaroni, P. Leclere, E. W. Meijer, A. Schenning, *J. Am. Chem. Soc.* **2006**, *128*, 5923–5929.
[19] J. R. Matthews, F. Goldoni, A. P. H. J. Schenning, E. W. Meijer, *Chem. Commun.* **2005**, *0*, 5503–5505.
[20] Y. Takahashi, H. Tadokoro, *Macromolecules* **1973**, *6*, 672–675.
[21] B. Servet, S. Ries, M. Trotel, P. Alnot, G. Horowitz, F. Garneir, *Adv. Mater.* **1993**, *5*, 461–464.
[22] S. Hotta, Y. Ichino, Y. Yoshida, M. Yoshida, *J. Phys. Chem. B* **2000**, *104*, 10316–10320.
[23] J. L. Mynar, T. Yamamoto, A. Kosaka, T. Fukushima, N. Ishii, T. Aida, *J. Am. Chem. Soc.* **2008**, *130*, 1530–1531.

© 2013 Wiley-VCH Verlag GmbH & Co. KGaA, Weinheim